



1 **Linear and Non-linear Stability Analysis of the Rate and State Friction
2 Model with Three State Variables**

3 Nitish Sinha, Arun K. Singh
4 Visvesvaraya National Institute of Technology, Nagpur-440010, INDIA
5 nitishme08@gmail.com aksinghb@gmail.com

6 **Abstract**

8 In this article, we study linear and non-linear stability of the three state variables rate and state
9 friction (3sRSF) model with spring-mass sliding system. Linear stability analysis shows that
10 critical stiffness, at which dynamical behaviour of the sliding system changes, increases with
11 number of state variables. The bifurcation diagram reveals that route of chaos is period
12 doubling and this has also been confirmed with the Poincaré maps. The present system is
13 hyperchaos since all Lyapunov exponents are positive. It is also established that the 3sRSF
14 model is more chaotic than corresponding to the 2sRSF model. Finally, the implication of the
15 present study is also discussed.

16 **1. Introduction**

17 One of the most important applications of friction in recent decades is in understanding the
18 sliding dynamics of earthquake faults (Brace and Byerlee, 1966; Dieterich, 1979; Rice and
19 Ruina, 1983). It is believed that the stick-slip process along the earthquake faults results in
20 earthquakes. Researchers use rate and state friction(RSF) model oftenly to explain the
21 earthquake process (Brace and Byerlee, 1966; Dieterich, 1979; Rice and Ruina, 1983). The
22 RSF model was proposed by Dieterich (1979,1981), Ruina (1983) and Ruina and Rice (1983).
23 Although the RSF model is an empirical model, its genesis has been explained using the
24 Eyering's rate reaction theory (Rice et. al., 2001). Classical Amontons-Coulombs' (AC) laws
25 are widely used for explaining variety of friction based phenomena of hard solids
26 (Persson,2000). Nonetheless these friction laws do not explain many observations for
27 instance increase in friction with time of contact and sliding velocity, more significantly,
28 stiffness dependence of stick-slip behavior etc. (Rice and Ruina,1983). In fact, these



1 limitations of the AC laws led to the proposal of the modified friction model which is known
2 as the rate and state friction (RSF) model. According to this friction model of hard solids such
3 as rock solids depends on the “slip rate” as well as the “state” of the sliding surfaces (Rice and
4 Ruina,1983; Ruina,1983). Although one state variable explains well the stiffness dependence
5 of stick-slip oscillatory motion of a sliding mass, it doesn’t explain its chaotic behavior. As a
6 result, one state variable RSF law has been modified by introducing an additional state
7 variable by believing that chaos is a manifestation of more complex friction processes at the
8 slip interface. This observation led to the proposal of the two state variables rate and state
9 dependent friction (2sRSF) model. The 2sRSF model shows the chaotic behavior (Ruina,
10 1983; Gu et. al., 1984; Gu and Wong, 1994; Zhiern and Dangmin, 1994; Niu and Chen, 1995;
11 Becker, 2000; Gao, 2013). It arises naturally a question what happens to the 2sRSF model if
12 one more state variable is added in this friction model. In this article we have studied
13 numerically linear and nonlinear dynamics of the three state variables rate and state
14 friction(3sRSF) with spring-mass sliding system. The results are also compared with the
15 corresponding two state variables rate and state friction (2sRSF) model.

16 Chaos is defined as “Aperiodic long-term behavior in a deterministic system that exhibits
17 sensitive dependence on initial conditions” (Strogatz,1994). The conditions for a continuous
18 dynamical system to be chaotic are that the governing differential equation must possess at
19 least three independent variables, and also show the dependence on initial conditions
20 (Devany,1989). There are many well known and extensively studied chaotic systems in
21 literature for example Duffing oscillator, Lorenz system, Rössler system etc. (Strogatz,1994).
22 Moreover, phase plot, Poincaré maps, bifurcation diagram, Lyapunov exponents etc. are the
23 numerical tools which are widely used for studying chaotic behavior of a dynamical system.
24 Rössler introduced the concept of hyperchaos by modifying one of the simplest chaotic
25 models (Rössler,1979). The general conditions for the hyper-chaos are that the system of



1 differential equations should have at least four independent variables and the system must
2 also be dissipative (Wang and Wang,2008; Chen et. al., 2006). Moreover, the Lyapunov
3 exponents of the dynamical system must show at least two positive, one zero and one negative
4 (Niu and Chen,1995). Further, the sum of all Lyapunov exponents must be negative
5 (Moghtadaei and Goplaegani,2012). In additions to these conditions, the phase plot should
6 also show twisting structure in the chaotic behavior (Moghtadaei and Goplaegani, 2012).
7 Notwithstanding the aforementioned conditions for hyperchaos, there are dynamical systems
8 which have been claimed to be hyper chaos. For example, Oteski et al. (2015) have claimed
9 that an air-filled differentially heated cavity to be hyperchaotic on the basis of all positive
10 Lyapunov exponents(LEs). In the present 3sRSF model as well, we will establish numerically
11 that all LEs are positive hence the 3sRSF dynamical system to be hyperchaotic.
12 In literature majority of study has been done with one state variable based RSF law (Ranjith
13 and Rice, 1999). The reason may be attributed to the fact that one state variable based friction
14 law is enough to explain the stick-slip phenomenon or frictional instability of hard surfaces.
15 Gu et al. (1984) have studied numerically the linear and non-linear behaviour of the spring-
16 mass slider with the 1sRSF model as well as the 2sRSF model. They have reported stick-slip
17 behavior with 1sRSF model while the 2sRSF model shows the period doubling as well as
18 chaotic behaviour. Gu and Wong (1992) have carried out linear and nonlinear stability
19 analysis with both the1sRSF and 2sRSF models using the tools phase portraits, time series,
20 and bifurcation diagrams. They have established that the most significant parameter is spring
21 stiffness which controls the stability of the sliding mass. Zhiren and Dangmin (1994,1995)
22 have carried out the numerical simulations of 2sRSF model with the slip law, and they
23 observed that the sliding system shows the quasi-periodic to chaotic behaviour upon decrease
24 in spring stiffness even in the absence of inertia that is, under the quasistatic conditions. They
25 have also estimated the Lyapunov exponents as well as Lyapunov dimensions to confirm the



1 evidence of chaotic behaviour of the system (Niu and Chen, 1995). Xuejun(2013) has
2 investigated the stability of the 2sRSF and finds the period doubling route to chaos. Wang
3 (2002,2009) has pointed out that the “slip” and “slowness” laws differ in high velocity
4 regime but not in the low velocity sliding regime. In recent times the 2sRSF model has been
5 used to validate the experimental data concerning rock friction at high temperature in the
6 framework of the 2sRSF(Liu, 2007 King and Marone,2012). Nontheless these researchers
7 have not reported any evidence of chaotic behavior in the experiments at high temperature.
8 The present analysis is related with the three state variable RSF model i.e., the 3sRSF model.
9 The organization of the paper is as following. First we have derived governing differential
10 equations of the spring-mass sliding system with 3sRSF in non-dimensional form following
11 the same procedure as was done by Xuejun[2013]. It is then linear stability of Eq. (4) is
12 carried out by linearizing about steady state or equilibrium points. The expression for critical
13 stiffness is also derived using Routh- Hurwitz criterion (Persson,2000). The physical meaning
14 of the critical stiffness is that at this value of stiffness the sliding behavior changes from
15 unstable to stable sliding or vice versa. The non-linear analysis of Eq. (4) is also carried out in
16 detail with different tools such as phase plot, Poincaré maps, bifurcation diagram, Lyapunov
17 exponents and Lyapunov dimensions. Finally a comparative study is also done between
18 2sRSF and 3sRSF models to justify the present results.

19 **2. Modelling of Spring-mass system with three state variables friction law**

20 According to the rate and state friction(RSF) model, frictional stress ‘ τ ’ of a sliding hard
21 surface depends on sliding velocity ‘ v ’ and state variable ‘ θ ’ (Ruina, 1983). Based on the
22 experimental observations Dieterich(1978), Ruina(1980,1983), Ruina and Rice(1983)
23 proposed the following empirical relation

24
$$\tau = \tau^* + \theta_i + A \ln \frac{v}{v^*}, \text{ and } \frac{d\theta_i}{dt} = -\frac{v}{L_i} \left[\theta_i + B_i \ln \frac{v}{v^*} \right]. \quad (1)$$



1 where θ_i is number ($i=1,2,3\dots$) of state variables, B_i are L_i are the constants. Further ' τ^* ' and
 2 ' v^* ' are reference frictional shear stress and shear velocity respectively. The system of
 3 differential equations in Eq.(1) with three state variables are expanded as

$$4 \quad \begin{aligned} \tau &= \tau^* + \theta_1 + \theta_2 + \theta_3 + A \ln \frac{v}{v^*}, \& \frac{d\theta_1}{dt} &= -\frac{v}{L_1} \left[\theta_1 + B_1 \ln \frac{v}{v^*} \right]. \\ \frac{d\theta_2}{dt} &= -\frac{v}{L_2} \left[\theta_2 + B_2 \ln \frac{v}{v^*} \right], \& \frac{d\theta_3}{dt} &= -\frac{v}{L_3} \left[\theta_3 + B_3 \ln \frac{v}{v^*} \right]. \end{aligned} \quad (2)$$

5 Dieterich(1979), Ruina(1983) have proposed two laws governing the "state" of the sliding
 6 surfaces which are known as the Ruina-Rice slip law or simply slip law and Dieterich-Ruina
 7 ageing law or ageing law [3]. It is important to note that the, unlike ageing law, the slip law of
 8 the RSF model shows chaotic behaviour (King and Marone,2012). The reason for this
 9 contradictory observation is not yet reported in literature.

10 In order to study the 3sRSF model, we have also used the spring-mass sliding system under
 11 the quasi-static conditions. The free end of the spring having spring constant $k(Pa m^{-1})$ is
 12 being pulled constantly with a constant pulling velocity ' v_0 ' as a result the rate of change of
 13 friction at the sliding interface is given by

$$14 \quad \frac{d\tau}{dt} = k(v_0 - v). \quad (3)$$

15 The non-dimension form of above set of Eqs.(1-5) are expressed by introducing non-
 16 dimension variables as velocity ϕ , shear stress f , state variables $\hat{\theta}_1$, and $\hat{\theta}_2$, time T , pulling
 17 velocity ϕ_0 , spring stiffness K

$$18 \quad \begin{aligned} f &= \frac{\tau - \tau^*}{A}, \& \phi &= \ln \frac{v}{v^*}, \& \hat{\theta}_1 &= \frac{\theta_1}{A}, \& \hat{\theta}_2 &= \frac{\theta_2}{A}, \& T &= \frac{v^*}{L_1} t, \& \beta_1 &= \frac{B_1}{A}, \& \beta_2 &= \frac{B_2}{A}, \& \beta_3 &= \frac{B_3}{A}, \& \rho &= \frac{L_1}{L_2}, \\ \rho_1 &= \frac{L_1}{L_3}, \& \phi_0 &= \ln \frac{v^0}{v^*}, \& K &= k \frac{L_1}{A}. \end{aligned}$$



1 Non-dimensional form of the system of differential equations Eq.(4) is obtained using Eqs. (2-
 2 3). After having eliminated the third state variable $\hat{\theta}_3$, we get the following system of
 3 differential equations:

$$4 \quad \begin{cases} \frac{d\phi}{dT} = e^\phi \left[(1 - \rho_1) \hat{\theta}_1 + (\rho - \rho_1) \hat{\theta}_2 + (\beta_1 + \rho\beta_2 + \rho_1\beta_3 - \rho) \phi + \rho_1 f - K \right] + K e^{\phi_0} \\ \frac{df}{dT} = K (e^{\phi_0} - e^\phi) \\ \frac{d\hat{\theta}_1}{dT} = -e^\phi (\hat{\theta}_1 + \beta_1 \phi) \\ \frac{d\hat{\theta}_2}{dT} = -\rho e^\phi (\hat{\theta}_2 + \beta_2 \phi) \end{cases} \quad (4)$$

5 It may be noted that Eq.(4) is having four variables i.e, four dimensional system, thus we
 6 investigate the possibility of hyperchaos in Eq.(4).

7 **3.0.Results and Discussion**

8 **3.1.Linear Stability analysis**

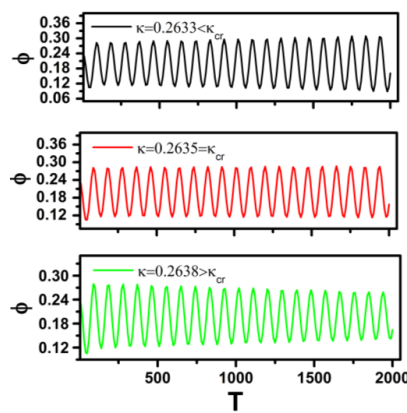
9 Linear stability of the spring-mass model is done about steady state or equilibrium
 10 point(Strogatz, 1994). The equilibrium or fixed points are obtained by equating the equations
 11 to zero. The equilibrium points of Eq.(4) are obtained as

$$12 \quad \phi_{ss} = \phi_0, \quad \theta_{1ss} = -\beta_1 \phi_0, \quad \hat{\theta}_{2ss} = -\beta_2 \phi, \quad \text{and} \quad f_{ss} = \left(\frac{\rho}{\rho_1} - \beta_1 - \beta_2 - \beta_3 \right) \phi_0 \quad (5)$$

13 The charactersticequation $|J_0 - \lambda I| = 0$,is expanded for polynomial equation in terms of eigen
 14 value λ . where J_0 is Jacobian matrix of Eq.(4) about the steady state and I is identity matrix.
 15 Routh-Hurwitz criterion is used to obtain critical stiffness k_{cr} at which sliding behaviour of
 16 the spring-mass system changes. Other details about evaluating k_{cr} is given in appendix-I.
 17 The physical significance of k_{cr} is that the sliding system changes its behaviour from unstable
 18 to stable sliding for spring stiffness larger than k_{cr} (Gu et. al., 1984; Ranjith and Rice,1999).
 19 For instance, Fig.1 presents the results that the sliding system is dynamically unstable for



1 stiffness $k = 0.2633$ and neutral for critical stiffness $k_{cr} = 0.2635$ and stable for stiffness
 2 $k_{cr} = 0.2638$. The value of critical stiffness is evaluated numerically using the expression for
 3 critical stiffness given in Appendix-I. Noting that the results in Fig.1 are in confirmation with
 4 the 1s RSF model (Ranjith and Rice,1999).

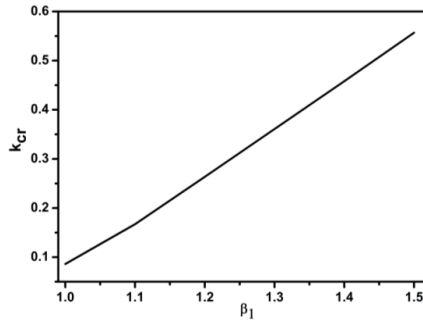


5
 6 Fig.1. Stiffness dependent sliding behavior of spring-mass for $\beta_1 = 1.2, \beta_2 = 0.84, \beta_3 = 0.38,$
 7 $\rho = 0.048$ and $\rho_1 = 0.034$ for initial condition $[0.19885, -1.00824, -0.23862, -0.167034]$.
 8
 9 **3.2. Effect of friction parameters on critical stiffness**

10 The effect of friction parameter such as β_1 is investigated on critical stiffness k_{cr} numerically.
 11 The values of friction parameters are considered the same as in literature[Rice and Ruina,1983;
 12 Gu. et. al.,1984]. However numerical values of additional parameters β_3 and ρ_1 in the 3sRSF
 13 model are estimated on the basis of the reported values in literature (Gu. et. al., 1984) For
 14 instance, friction parameter β decreases if friction law is modified from one state variable to
 15 two state variables. The result in Fig.2 shows that k_{cr} increases linearly with β_1 . This linear
 16 behaviour is also seen with the 2sRSF law though we are not presenting the results here. The
 17 dependence of critical stiffness in the 3sRSF model with respect to variables, for instance
 18 β_2, β_3, ρ and ρ_1 , is also linear though we have not presented the results here.



1



2 Fig.2. Effect of friction parameter β_1 on critical stiffness k_{cr} for $\beta_2 = 0.84$, $\beta_3 = 0.38$,
 3 $\rho = 0.048$ and $\rho_1 = 0.034$.

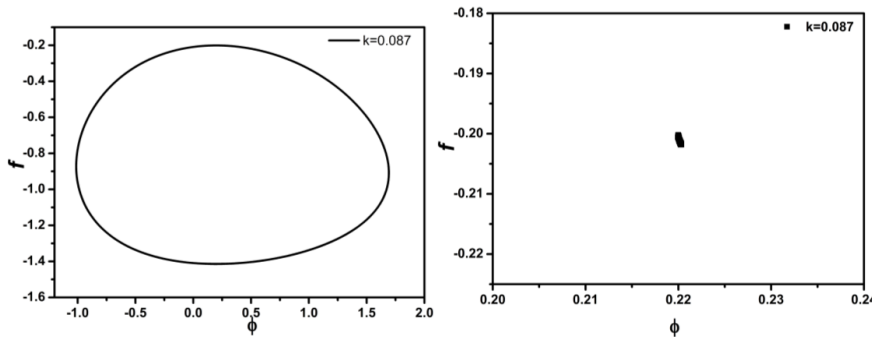
4

5

6 **3.3. Nonlinear stability analysis**

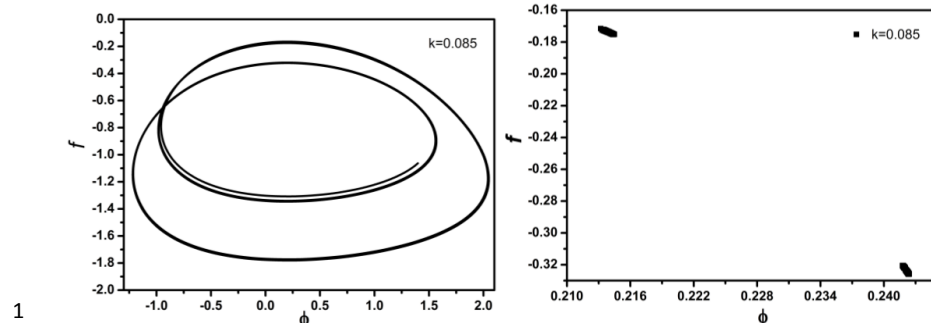
7 Motivated from linear stability analysis, we have also carried out non-linear stability of the
 8 system of governing differential equations in Eq.(4). This is solved with MATLAB[®] using
 9 *ode23s* solver for ordinary differential equations. Fig.3 shows the single orbit in phase
 10 portrait, which means the system behaviour is periodic at spring stiffness $k = 0.087$. This has
 11 also been confirmed using Poincaré section which shows single point in the map in Fig.3.

12



13 Fig.3 phase diagram(left) f vs. ϕ and Poincaré section(right) for $k = 0.087$, $\beta_1 = 1.0$,
 14 $\beta_2 = 0.84$, $\beta_3 = 0.38$, $\rho = 0.048$ and $\rho_1 = 0.034$ for initial condition $[0,0,0,0]$.
 15

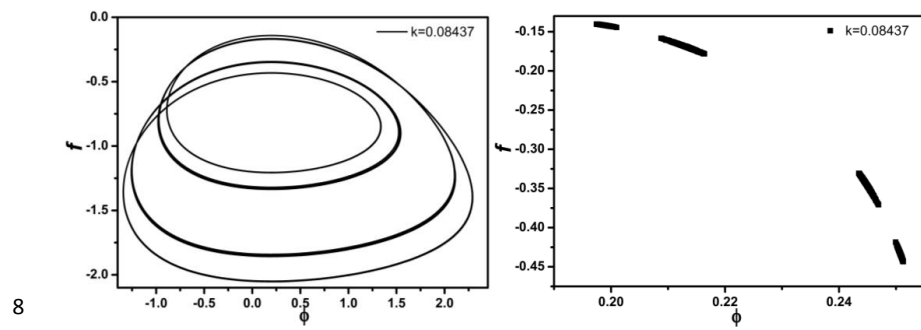
16 Now upon lowering the magnitude of spring stiffness to $k = 0.085$, Fig.4 shows the evidence
 17 of period doubling and this phenomena is also confirmed by the Poincaré map. As Poincaré
 18 section in Fig.4 shows two points.



1 Fig.4 phase diagram f vs. ϕ and corresponding Poincaré section for $k = 0.085$, $\beta_1 = 1.0$,
 2 $\beta_2 = 0.84$, $\beta_3 = 0.38$, $\rho = 0.048$ and $\rho_1 = 0.034$ for initial condition [0,0,0,0].

3

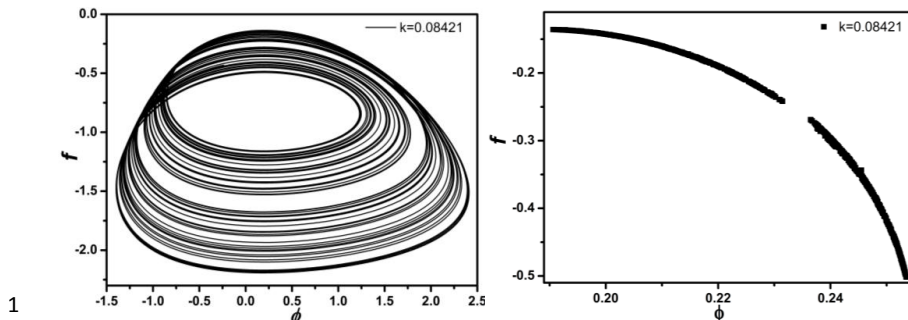
4
 5 As magnitude of stiffness decreases further to $k = 0.08437$, the dynamical behaviour of the
 6 system changes further. Now the phase portrait in Fig.5 results in period quadrupling and this
 7 is also confirmed in the corresponding Poincaré section in Fig.5.



8 Fig.5 phase diagram f vs. ϕ and corresponding Poincaré section for $k = 0.08437$, $\beta_1 = 1.0$,
 9 $\beta_2 = 0.84$, $\beta_3 = 0.38$, $\rho = 0.048$ and $\rho_1 = 0.034$ for initial condition [0,0,0,0].

10

11
 12 As the controlling parameter k decreases further, the 3sRSF leads the spring-mass system in
 13 chaos. For instance, Fig.6 presents the phase diagram and corresponding Poincaré section for
 14 $k = 0.08421$. The phase portrait shows infinite period with bounded orbits and the
 15 corresponding Poincaré section in the form of continuous line.

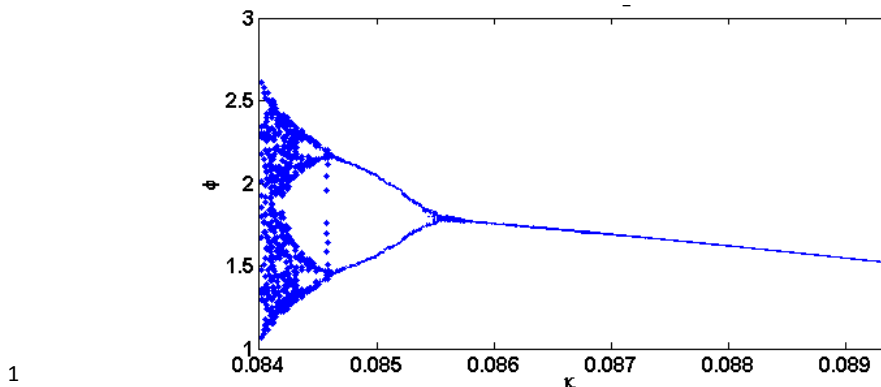


2 Fig.6 phase diagram f vs. ϕ and corresponding Poincaré section for $k = 0.08421$, $\beta_1 = 1.0$,
 3 $\beta_2 = 0.84$, $\beta_3 = 0.38$, $\rho = 0.048$ and $\rho_1 = 0.034$ for initial condition $[0,0,0,0]$.

4
 5 A physical significance of the present results is in nucleation of earthquake process. For
 6 instance, The phase portraits in Fig.3-6 show an interesting observation that frictional stress
 7 as well as corresponding slip velocity at the sliding interface changes from periodic to chaotic
 8 upon decreasing spring stiffness of the slider. This results in a direct surge of stress amplitude
 9 thus the nucleation of earthquake process occurs. This observation is similar to the chaotic
 10 nature of the sliding mass with the 2sRSF in which magnitude of the stress fluctuates
 11 considerably thus the earthquake nucleation begins (Becker, 2000).

12 **3.4 Bifurcation diagram**

13 The results in Figs.(3-6) have also been confirmed by the bifurcation diagram in shown Fig.7.
 14 In the bifurcation diagram the control parameter in the form of non-dimensional stiffness k
 15 decreases by a small step 10^{-6} from $k = 0.089$ to $k = 0.084$, the evolution of the system is
 16 initially periodic oscillation with increasing amplitude as evident in Fig.7. Upon further
 17 decrease in stiffness upto $k = 0.085$, the behaviour of the system changes to period doubling
 18 as obvious in Fig.7. If stiffness decreases to further lower value i.e., $k = 0.08437$, the system
 19 behaviour bifurcates to the period four (Fig.7). Finally the system results in chaotic behaviour
 20 at minimum stiffness $k = 0.08421$. These results are in confirmation with phase portraits and
 21 Poincaré section in Figs.(3-6).



1
2 Fig.7 Bifurcation diagram for spring stiffness $k = 0.87$ to 0.084 , $\beta_1 = 1.0$, $\beta_2 = 0.84$,
3 $\beta_3 = 0.38$, $\rho = 0.048$ and $\rho_1 = 0.034$ for initial condition $[0,0,0,0]$.

4
5 Fig.7 also summarizes the variation of velocity amplitude with decreasing spring stiffness. It
6 is obvious that the overall velocity amplitude increase from periodic to chaotic way as
7 stiffness of the connecting spring decreases. This observation is consistent with the phase
8 plots in Figs.3-6.

9 **3.5 Lyapunov exponent and dimensions**

10 Lyapunov exponent(LE) is the most significant tool for investigating the dynamical behavior
11 of a physical system (Kaplan and Yorke, 1979). We have used the MATLAB® program for
12 evaluating the LE of the present dynamical system by Lyapunov Exponent Toolbox (LET),
13 which is developed by Steve SIU (1998). For the four-dimensional dissipative system, there
14 are three possible type of strange attractors such as the combination of Lyapunov spectra as
15 $(+, +, 0, -)$, $(+, 0, 0, -)$ and $(+, 0, -, -)$ (Wolf. et. al., 1985). If LE is negative the dynamical system is
16 stable with dissipative in nature, while the positive LE signifies the system become unstable
17 orbit or chaotic. However, LE with zero magnitude signifies the system is dynamically neutral
18 (Wolf. et. al., 1985).

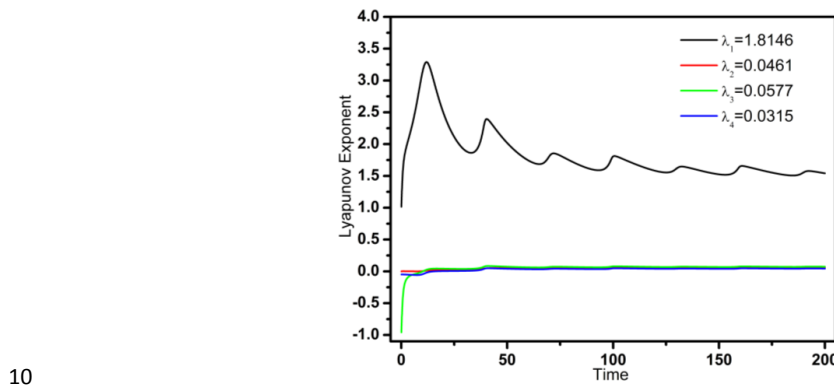
19 The present analysis of the 3sRSF model shows in Fig.8 that the magnitude of LEs are
20 $LE_1 = 1.8146$, $LE_2 = 0.0461$, $LE_3 = 0.0577$, $LE_4 = 0.0351$. This result confirms that the present
21 dynamical system is very similar to a hyperchaos as more than one Lyapunov exponents is



1 positive (Oteski. et. al., 2015). At the same time, the magnitude of three LEs are one order
 2 less than the remaining one. This result is in contrast with the 2sRSF in which results are one
 3 positive, one negative and one zero in magnitude (Niu and Chen,1995). The relationship
 4 between the Lyapunov exponents and fractal dimensions is established by Kaplan and
 5 Yorke(1979). They have proposed the Lyapunov or Kaplan-Yorke dimension D_{KY} which is

6 given by the formula: $D_{KY} = D + \frac{1}{|h_D + 1|} \sum_{i=1}^D h_i$

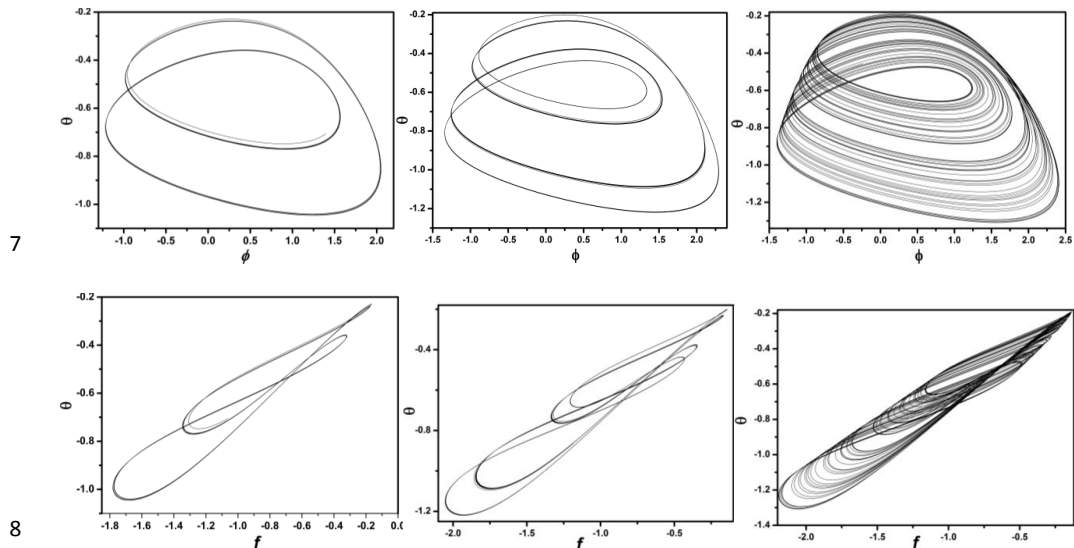
7 where D is the largest integer for which $\sum_{i=1}^D h_i > 0$. As a result, D_{KY} is a convenient
 8 geometrical measure of objects in phase space if Lyapunov exponents are known. The fractal
 9 dimension of the present dynamical system is calculated to be as 5.70.



10
 11 Fig.8.Lyapunov exponents vs. time for $k=0.08421$, $\beta_1 = 1.0$, $\beta_2 = 0.84$, $\beta_3 = 0.38$, $\rho = 0.048$
 12 and $\rho_1 = 0.034$ for initial conditions $[0,0,0,0]$
 13 The 3sRSF based quasistatic system also follows the universal period doubling route to chaos.
 14 The Feigenbaum number is estimated using given formula $\delta_n = (k_{n+1} - k_n)/(k_{n+2} - k_{n+1})$ where
 15 $n = 1, 2, 3, \dots$, this number should converge to Feigenbaum number 4.669201. we have
 16 calculated Feigenbaum universality constant for 3sRSF law and estimated to 3.9375. However
 17 this single value does not indicate the sign of convergence. It may be possible that



1 convergence for the bifurcation sequence to chaos for the friction model is different from the
 2 logistic map.
 3
 4 We have also investigated whether the present friction model fulfils the other conditions of
 5 hyperchaos. The hyperchaotic behavior in the form of phase portraits in Fig.9 shows the
 6 twisting nature of the phase diagram. This is also a feature of hyper chaos().



7
 8 Fig.9. Twisted phase diagram for stiffness value (a) $k = 0.085$, (b) $k = 0.08437$, (c)
 9 10 $k = 0.08421$ and $\beta_1 = 1.0, \beta_2 = 0.84, \beta_3 = 0.38, \rho = 0.048$ and $\rho_1 = 0.034$ for initial condition
 11 $[0,0,0,0]$.
 12

13 We have also compared the linear and non-linear behavior between the 2sRSF and the 3sRSF
 14 models. For instance, critical stiffness, at which dynamics of stick-slip motion changes,
 15 increases with number of state variables. Moreover, the route of chaos is same for both
 16 2sRSF and 3sRSF models, that is, period doubling. But period eight and period sixteen are
 17 not observed in the present system which is unlike to the 2sRSF model (Xuejun,2013).
 18 Moreover,LEs of the 2sRSF are reported to be one positive, one negative and one zero. The
 19 3sRSF model, in contrast, shows all four LEs are positive. This result has been confirmed



1 using magnitude of fractal dimension (FD). For example, FD of the 2sRSF is 2.11 which is
2 less than the FD of 3sRSF i.e., 5.7. Moreover, Poincaré section of the 3sRSF model is
3 slightly intricate than the 2sRSF model. On the basis of these evidences, it is established that
4 the 3sRSF model is more chaotic than the 2sRSF model.

5 **5. Conclusions**

6 We have established numerically that the three state variables based RSF model show the
7 chaotic behavior. All Lyapunov exponent is positive. The route of chaos is established to be
8 period doubling bifurcation. Moreover, critical stiffness of the dynamical system increases
9 with number of state variables. It is also observed that the 3sRSF is more chaotic than
10 corresponding to the 2sRSF. It is shown that the 3sRSF model is hyperchaotic as it exhibits
11 all positive Lyapunov exponents.

12 **References:**

13 Brace,W.F.,Byerlee,J.D.:Stick-slip as a Mechanism of earthquake,Science,153,990-992,1966
14 Chen,A.,Lu,J.,Lu,J.,Yu,S.:GeneratinghyperchaoticLü attractor via state feedback control,Physica A.
15 364,103–110,2006
16 Dieterich, J.D.:Modeling of rock friction:1.experimental results and constitutive equation, J.
17 Geophys.Res., 84(B5), 2161-2168,1979
18 Devany.R.:An introduction to chaotic dynamical system, est view press,1989
19 Feigenbaum,M.J.:Universal behavior in Nonlinear System. Physica.7D,16,1983
20 Gu, Y. and Wong, T.-F.:Nonlinear dynamics of the transition from stable sliding to cyclic stick-slip in
21 rock, in Nonlinear dynamics and predictability of geophysicalphenomena, vol. 8:3,
22 GeophysicalMonograph, edited by W.I.Newman, A. Gabriclov, and D. L. Turcotte, pp. 15-35,1994,
23 AGU, Washington, D.C.
24 Gu J.C., Rice,J.R., Ruina, A.L. and Tse, S.T.: Slip motion and stability of a single degree of freedom
25 elastic system with rate and state dependent friction. J. Mech. Phys. Solids.32, 167-196,1984
26 Jeen-HwaWang.:A Dynamic Study of Two One-State-Variable, Rate-Dependent, and State-
27 Dependent Friction Laws, Bulletin of the Seismological Society of America. 92,687-694,2002
28 Jeen-HwaWang.:A Numerical study of comparision of two one-state-variable, rate-and-state-
29 dependent friction evolution laws, Earthquake Science.22,197-204,2009



- 1 King,D.S.H.,Marone,C.:Frictional properties of olivine at high temperature with applications to the strength and dynamics of the oceanic lithosphere. *J. Geophys. Res.* 117, B12203,2012
- 2 Wolf, A., Jack, B.S., Harry, L. S., John, A. V.:Determineing Lyapunov exponents from a time series. *Physica*, 16D, 285-317,1985
- 3 Kaplan,J.L.,Yorke,J.A.:Chaotic behavior of multidimensional difference equation, in *Functional Differential Equation and Approximation of Fixed Points*, Vol. 730,Lecture Notes in Mathematics, edited by H.-O. Peitgen and H.-O. Walter, pp. 204-227,1979 Springer,Berlin
- 4 Marone, C.:Laboratory-derived friction laws and their application to seismic faulting, *Annual Review of Earth and Planetary science*,26 643-696,1998
- 5 Moghtadaei,M.,Goplayegani,M.R.H.:Complex dynamics behaviours of the complex Lorenz system, *ScientiaIranica* D.19(3),733-738,2012
- 6 Niu, Z.-B. and Chen, D.-M.:Lyapunov exponent and dimension of the strange attractor of elastic frictional system, *ActaSeimol. Sinica*.8,575-584,1995
- 7 O.E. Rossler.:An equation for Hyperchaos, *Physics Letters*.71A,2-3,1979
- 8 Oteski, L., Daguet, Y., Pastur, L., and Quèrè, P.L.:Quasiperiodic routes to chaos in confined two-dimensional differential convection., *Phys.Rev. E* ,92 043020,1-15,2015
- 9 Persson Bo. N. J.:Sliding friction physical principal and application,2nd ed., springer. Verlag Berlin Heidelberg New York,2000
- 10 Rice, J.R., Ruina, A.L.:Stability of steady frictional slipping. *J.Appl.Mech.*50, 343–349,1983
- 11 Ruina A.L.:slip instability and state variable friction laws. *B12*,88,10359-10370,1983
- 12 Rice,J.R, Lapusta,N.,Ranjith,K.: Rate and state dependent friction and the stability of sliding between elastically deformable solids. *Journal of the Mechanics and Physics of Solids*, 49 1865 – 1898,2001
- 13 Ranjith,K.,Rice,J.R.:Stability of quasi-static slip in a single degree of freedom elastic system with rate and state dependent friction" *Journal of the Mechanics and Physics of Solids*. 47, 1207-1218,1999
- 14 Roy, M.,Marone,C.:Earthquake nucleation on models faults with rate and state dependent friction: The effects of inertia, *J. Geophys. Res.*101,13919 – 13932,1996
- 15 Steven H. Strogatz.: Nonlinear dynamics and chaos,Perseus books publishing:Cambridge,MA,1994
- 16 Thorsten W. Becker.:Deterministic Chaos in two state-variable friction slider and effect of elastic itteraction,Geocomplexity and the Physics of Earthquakes. 120, 5,2000
- 17 Wang,X.,Wang,M.A.:Hyperchaos generated from Lorenz system, *Physica A*.387 (14), 3751–3758,2008
- 18 XuejunGao.:Bifurcation Behaviors of The two-state variable frictional law of a rock mass system, *Int. J Bifur. Chaos*.23,11,2013, DOI:10.1142/S0218127413501848



- 1 YajingLiu.:Physical Basis of Aseismic Deformation Transients in SubductionZones,PhD thesis,
- 2 Harvard University,2007
- 3 Zhiren, N. and Dangmin, C.:Period-Doubling Bifurcation and Chaotic Phenomena in a Single Degree
- 4 of Freedom Elastic System With A Two-State Variable Friction Law, in Nonlinear Dynamics and
- 5 Predictability of Geophysical Phenomena (eds W. I. Newman, A. Gabrielov and D. L. Turcotte),
- 6 American Geophysical Union, Washington, D. C.. doi: 10.1029/GM083p0075,1994
- 7 <http://in.mathworks.com/matlabcentral/fileexchange/233-let>

Appendix -I

10 It Jacobian matrix corresponding to the equilibrium point may be expressed as

11

$$12 J_0 = \begin{bmatrix} (\beta_1 + \rho\beta_2 + \rho_1\beta_3 - \rho)e^{\phi_0}, \rho e^{\phi_0}, (1 - \rho_1)e^{\phi_0}, (\rho - \rho_1)e^{\phi_0} \\ -Ke^{\phi_0}, 0, 0, 0 \\ -\beta_1 e^{\phi_0}, 0, -e^{\phi_0}, 0 \\ -\rho\beta_2 e^{\phi_0}, 0, 0, -\rho e^{\phi_0} \end{bmatrix}_{(\phi_{ss}, \hat{\theta}_{1ss}, \hat{\theta}_{2ss}, f_{ss})}$$

13 The polynomial equation containing the eigen values in term of λ is obtained from the
 14 expansion of the above Jacobian matrix as following

$$15 \lambda^4 + e^{\phi_0} (1 + \rho + \rho_1 + K - \beta_1 - \rho\beta_2 - \rho\beta_3) \lambda^3 + \\ e^{2\phi_0} (K + \rho + \rho_1 + \rho\rho_1 + 2K\rho - \rho\beta_1 - \rho\beta_2 - \rho_1\beta_1 - \rho\beta_3 - \rho\rho_1\beta_2 - \rho\rho_1\beta_3) \lambda^2 + \\ e^{3\phi_0} (2K\rho + \rho\rho_1 + \rho\rho_1\beta_1 - \rho\rho_1\beta_2 - \rho\rho_1\beta_3 + K\rho^2) \lambda + e^{4\phi_0} K\rho^2 = 0$$

$$s_0\lambda^4 + s_1\lambda^3 + s_2\lambda^2 + s_3\lambda + s_4 = 0$$

where:

$$s_0 = 1$$

$$16 s_1 = e^{\phi_0} (1 + \rho + \rho_1 + K - \beta_1 - \rho\beta_2 - \rho\beta_3)$$

$$s_2 = e^{2\phi_0} (K + \rho + \rho_1 + \rho\rho_1 + 2K\rho - \rho\beta_1 - \rho\beta_2 - \rho_1\beta_1 - \rho\beta_3 - \rho\rho_1\beta_2 - \rho\rho_1\beta_3)$$

$$s_3 = e^{3\phi_0} (2K\rho + \rho\rho_1 + \rho\rho_1\beta_1 - \rho\rho_1\beta_2 - \rho\rho_1\beta_3 + K\rho^2)$$

$$s_4 = e^{4\phi_0} K\rho^2$$

17 The Routh-Hurwitz criterion is used to get the condition for stability of the present friction
 18 model. The characteristic polynomial equation is obtained as $s_0\lambda^4 + s_1\lambda^3 + s_2\lambda^2 + s_3\lambda + s_4 = 0$.
 19 After applying the Routh-Hurwitz criteria $s_1s_2 - s_0s_3 = 0$ and $s_1s_2s_3 - s_0s_3^2 - s_4s_1^2 = 0$. These
 20 non-linear algebraic equations are in turn, solved numerically for evaluating critical stiffness.

21